ChemPubSoc Europe

DOI: 10.1002/chem.201600294

CHEMISTRY A European Journal Full Paper

Structure Elucidation

Montecrinanes A–C: Triterpenes with an Unprecedented Rearranged Tetracyclic Skeleton from *Celastrus vulcanicola*. Insights into Triterpenoid Biosynthesis Based on DFT Calculations

Martín Purino,[a] Alejandro E. Ardiles,[a, b] Oliver Callies,[a] Ignacio A. Jiménez,[a] and Isabel L. Bazzocchi*[a]

Abstract: Three new triterpenoids with an unprecedented 6/6/6/6-fused tetracyclic carbon skeleton, montecrinanes A–C (**1**–**3**), were isolated from the root bark of *Celastrus vulcanicola*, along with known *D*:*B*-friedobaccharanes (**4**–**6**), and lupane-type triterpenes (**7**–**12**). The stereostructures of the new metabolites were elucidated based on spectroscopic (1D and 2D NMR) and spectrometric (HR-EIMS and HR-ESIMS) techniques. Their absolute configurations were determined by both NMR spectroscopy, with (*R*)-(−)-α-methoxyphenylacetic acid as a chiral derivatizing agent, and biogenetic considerations. Biogenetic pathways for montecrinane and *D*:*B*-friedobaccharane skeletons were proposed and studied by DFT methods. The theoretical results support the energetic feasibility of the putative biogenetic pathways, in which the 1,2-methyl shift from the secondary baccharenyl cation represents a novel and key reaction step for a new montecrinane skeleton.

Introduction

Plant triterpenoids are pharmacologically active and structurally diverse natural products, which biogenetically originate from a common precursor, 2,3-(*S*)-oxidosqualene, through enzyme-initiated cation–olefin cyclization.[1] Regio- and stereochemical alternatives that are produced in the cyclization–rearrangement process can generate over 100 different skeletal types, which are subsequently modified by cytochrome P450s, dehydrogenases, reductases, and other modification enzymes to produce more than 20 000 triterpenoids.[2] They contain mono- to pentacyclic structures,[3] but the most frequently occurring are pentacyclic 6/6/6/6/6 and 6/6/6/6/5 systems, and the tetracyclic 6/6/6/5 system.

The 6/6/6/6 tetracyclic triterpenoids are rare in nature because few natural products with baccharane, *D*:*B*-friedobaccharane, lemmaphyllane, or shionane skeletons have been reported. The first 6/6/6/6 baccharane triterpene reported was baccharis oxide isolated from *Baccharis halimiolia*,[4,5] and subsequently, related metabolites have been isolated from different species.[6–12] The first members of triterpenes with a *D*:*B*-friedobaccharane framework (leonal and baruol (**4**)) were isolated from species of Celastraceae (*Maytenus blepharodes* and *M. chiapensis*).[13] Later, Zhang et al. reported three other new metabolites from *Salacia chinensis* (Celastraceae).[14] As for lemmaphyllane-type triterpenes, only two metabolites have been reported: lemmaphylla-7,21-diene,[15] and 3β-hydroxy-lemmaphylla-7,21-diene.[16] Regarding shionanes, the first example reported was russulaflavidin, which was isolated from *Russula flavida*,[17] and afterwards, another three were isolated from the rhizome of *Aster tataricus*.[18]

The enzymes that catalyze the formation of triterpenoids are known as triterpene synthases,[1] and their high stereospecificity and selectivity lead to one of the most complex reactions occurring in nature.[19] The first plant oxidosqualene synthase/cyclase (OSC) reported to yield a triterpene with a 6/6/6/6 tetracyclic system was baruol synthase (BARS1) from *Arabidopsis thaliana*, which produced **4** (90%) and 22 minor products.[20] Subsequently, baccharis oxide synthase (BOS) cloned from *Stevia rebaudiana*[5] and an *A. tataricus* OSC, yielding shionane as the major product, were reported.[21]

In recent years, the commercial significance of terpenoids as added-value products[22] has sparked interest in characterizing the genes and enzymes involved,[23] as well as in strategies to elucidate new triterpene biosynthetic pathways.[24] Furthermore, due to the lack of experimental information at the molecular level, quantum chemical calculation studies provide information to understand the complexity of the reactions.[25,26]

Celastraceae species are a common source of pentacyclic triterpenoids, including ursane, lupane, oleanane, and friedelane-type triterpenoids, whereas reports on taraxerane, glutinane,

[a] Dr. M. Purino, Dr. A. E. Ardiles, Dr. O. Callies, Dr. I. A. Jiménez, Prof. I. L. Bazzocchi
Instituto Universitario de Bio-Orgánica "Antonio González" and Departamento de Química, Universidad de La Laguna
C/Astrofísico Francisco Sánchez 2, 38206, La Laguna, Tenerife (Spain)
E-mail: ilopez@ull.es

[b] Dr. A. E. Ardiles
Departamento de Química, Facultad de Ciencias
Universidad de Chile, Las Palmeras 3425, Ñuñoa, Santiago (Chile)

Supporting information for this article is available on the WWW under http://dx.doi.org/10.1002/chem.201600294.

and dammarane compounds are scarce.[27] However, *Cassine xylocarpa*, a Salvadorian plant species, mainly biosynthesizes a small group of triterpenoids with an olean-18-ene backbone.[28] Moreover, species of this family are the first reported sources of *D*:*B*-friedobaccharanes, the biosynthetic origin of which has been postulated from the *D*:*B*-friedobaccharenyl cation; an intermediate between baccharane and shionane series.[13,29] Thus, the characterization of chemically novel triterpenoids from Celastraceae species could shed light on their biosynthetic biodiversity.

Previously, bioactive dihydro-β-agarofuran sesquiterpenes[30–33] and friedelane,[34,35] glutinane, olean-12-ene,[36] and *D*:*B*-friedobaccharane triterpenoids[29] from *Celastrus vulcanicola* were reported. Herein, we report the isolation and stereostructure of three triterpenoids with an unprecedented tetracyclic 6/6/6/6 backbone, named montecrinanes A–C (**1**–**3**), along with three known biosynthetic related *D*:*B*-friedobaccharanes (**4**–**6**), and six known lupane-type triterpenes (**7**–**12**). A plausible biosynthetic pathway for the structurally unique montecrinane framework was proposed and supported by DFT calculations. Finding novel carbon skeletons in natural products research is not common, and therefore, the isolation of a new core may be indicative of alternative pathways for triterpene biosynthesis.

Results and Discussion

Structural determination

The hexanes/Et_2O extract of the root bark of *C. vulcanicola*, a Salvadorian Celastraceae species, was subjected to multiple chromatographic steps, involving vacuum liquid chromatography (VLC), medium-pressure liquid chromatography (MPLC), and preparative TLC to yield three new triterpenoids, **1**–**3**, along with the known related compounds, **4**,[13] leonatriol (**5**),[29] and leonatriolone (**6**).[29] Moreover, six known pentacyclic lupane triterpenes (Figure 1) were isolated and identified as nepeticin (**7**),[37] 2α,3β-dihydroxy-lup-20(29)-ene (**8**),[37] 3β,6β-dihydroxy-lup-20(29)-ene (**9**),[38] betulin (**10**),[37] 6β,28-dihydroxy-3-oxolup-20(29)-ene (**11**),[37] and 6β-hydroxy-3-oxolup-20(29)-en-28-oic acid (**12**)[39] by comparison of their spectral data with values reported in the literature. The structures of the new compounds were deduced as described below.

Compound **1** was isolated as a colorless amorphous solid, with a specific rotation of -58.6° ($c=0.38$ in $CHCl_3$). The HR-EIMS data show a molecular ion $[M]^+$ at *m/z* 440.3654, which indicates a molecular formula of $C_{30}H_{48}O_2$ that requires 7 indices of hydrogen deficiency. The EIMS results reveal signals attributable to alcohol (*m/z* 422 $[M^+-18]$) and methyl (*m/z* 407 $[M^+-18-15]$) functions, and the IR spectrum presents characteristic absorption bands for hydroxyl ($\tilde{\nu}=3455\ cm^{-1}$), carbonyl ($\tilde{\nu}=1708\ cm^{-1}$), and alkene ($\tilde{\nu}=1459\ cm^{-1}$) groups. The ^1H NMR spectrum (Table 1) contains eight methyl signals, including two downfield singlets ($\delta_H=1.62$ (29-CH_3), 1.71 ppm (30-CH_3)), and a doublet signal at $\delta_H=0.87$ ppm (d, $J_{28,18}=6.5$ Hz; 28-CH_3). Moreover, characteristic signals of methylene protons adjacent to a carbonyl group at $\delta_H=2.28$ (overlapping signal; $H_{2\alpha}$) and 2.78 ppm (dt, $J_{2\beta,1\beta}=5.5$ Hz, $J_{2\beta,1\alpha}=14.4$ Hz; $H_{2\beta}$), one hydroxymethine group at $\delta_H=4.20$ ppm (dd, $J_{15\alpha,16\alpha}=5.8$ Hz, $J_{15\alpha,16\beta}=9.2$ Hz; H15), and two olefinic protons at $\delta_H=5.11$ (t, $J_{21,20}=6.9$ Hz; H21) and 5.83 ppm (dd, $J_{7,6}=3.1$, 6.4 Hz; H7) were observed. The edited HSQC and the broadband-decoupled ^{13}C NMR spectra established that compound **1** had 30 carbon atoms classified by DEPT experiments as eight methyl, eight methylene, seven methine, and seven quaternary carbon atoms. Further analysis revealed a carbonyl carbon signal at $\delta_C=216.7$ ppm (C3), four sp^2-carbon atoms at $\delta_C=118.5$ (7-CH), 124.9 (21-CH), 131.2 (C22) and 144.4 ppm (C8); this suggested two trisubstituted double-bond functions and a methine carbon bonded to oxygen ($\delta_C=76.7$ ppm (15-CH)) in a triterpene scaffold. These data indicate that compound **1** is a triterpene containing four carboxylic rings as a scaffold. 1D and 2D NMR spectroscopy experiments allow detailed structure and complete ^1H and ^{13}C NMR signal assignments (Table 1 and Figures, Sections A1–A4 in the Supporting Information). Thus, the ^1H NMR spectroscopy data, in combination with COSY and TOCSY experiments, enable us to draw substructures A–D, with the identification of four spin systems. Three of those are typi-

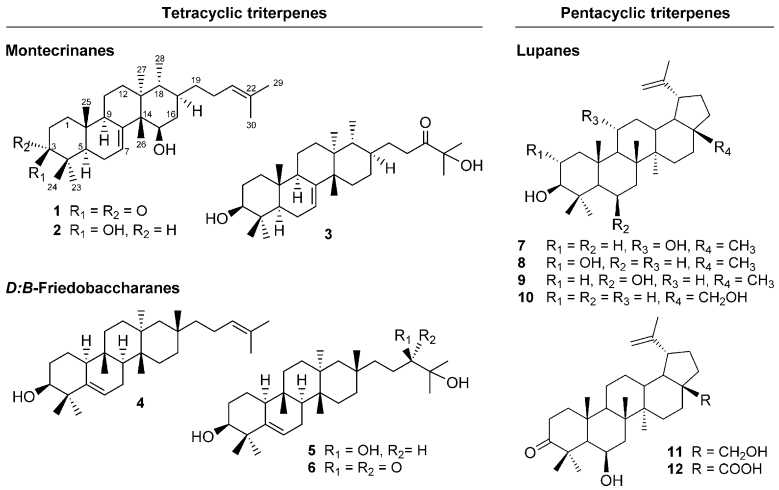

Figure 1. Structure of montecrinanes A–C (**1**–**3**), *D*:*B*-friedobaccharanes (**4**–**6**), and lupane triterpenes (**7**–**12**) isolated from *C. vulcanicola*.

Table 1. NMR spectroscopic data[a] for montecrinanes A (**1**), B (**2**), and C (**3**); coupling constants are given in Hz in parentheses.

Position	Montecrinane A (**1**)		Montecrinane B (**2**)		Montecrinane C (**3**)	
	δ_H[b]	δ_C[c]	δ_H[b]	δ_C[c]	δ_H[b]	δ_C[c]
1	1.49 dt (4.2, 14.4), 2.00	38.5 t	1.15 dt (4.3, 14.2), 1.71	37.2 t	1.15 dt (4.3, 14.3), 1.69	37.2 t
2	2.28, 2.78 dt (5.5, 14.4)	34.9 t	1.62, 1.70	27.7 t	1.63, 1.68	27.7 t
3		216.7 s	3.27 dd (3.9, 11.3)	79.2 d	3.27 dd (4.3, 11.5)	79.2 d
4		47.9 s	–	39.0 s		38.9 s
5	1.75 dd (6.2, 11.3)	52.3 d	1.34	50.6 d	1.34 dd (5.6, 12.3)	50.6 d
6	2.14	24.3 t	2.01, 2.14	23.9 t	1.99, 2.17	23.9 t
7	5.83 dd (3.1, 6.4)	118.5 d	5.76 dd (3.1, 6.4)	118.0 d	5.28 dd (3.0, 6.6)	118.0 d
8		144.4 s		144.3 s		145.6 s
9	2.28	48.7 d	2.18	49.1 d	2.22	48.8 d
10		35.0 s		34.9 s		34.9 s
11	1.60	18.3 t	1.55	18.1 t	1.55	18.1 t
12	1.61, 1.89	34.6 t	1.61, 1.88	34.7 t	1.71, 1.48	33.7 t
13				44.2 s		43.5 s
14		52.2 s		52.2 s		51.2 s
15	4.20 dd (5.8, 9.2)	76.7 d	4.19 dd (5.8, 9.2)	76.7 d	1.53, 1.82 dd (10.4, 13.4)	33.9 t
16	1.71, 1.97	40.5 t	1.70, 1.95	40.5 t	1.31, 1.96	28.4 t
17	1.34	35.7 d	1.33	35.7 d	1.44	35.5 d
18	1.56	50.8 d	1.56	50.7 d	1.52	53.2 d
19	1.04, 1.40	36.1 t	1.04, 1.40	36.1 t	1.24, 2.01	28.9 t
20	1.89, 2.05	24.9 t	2.05	24.9 t	2.51 ddd (5.3, 9.5, 15.6) 2.60 ddd (6.5, 9.5, 15.6)	32.9 t
21	5.11 t (6.9)	124.9 d	5.11 t (6.9)	125.0 d		214.8 s
22		131.2 s		131.2 s		76.2 s
23	1.07 s	24.5 q	1.00 s	27.6 q	0.99 s	27.6 q
24	1.14 s	21.5 q	0.89[b] s	14.7 q	0.88 s	14.7 q
25	1.03 s	12.8 q	0.78 s	13.1 q	0.77 s	13.1 q
26	1.10 s	19.3 q	1.07 s	19.2 q	1.01 s	27.3 q
27	0.89 s	22.1 q	0.89 s	22.1 q	0.86 s	21.9 q
28	0.87 d (6.5)	18.1 q	0.88 d (6.5)	18.2 q	0.87 d (6.0)	18.5 q
29	1.62 s	17.6 q	1.62 s	17.7 q	1.41 s	26.6 q
30	1.71 s	25.7 q	1.71 s	25.8 q	1.41 s	26.6 q

[a] Spectra were recorded in $CDCl_3$ at 25 °C (^1H 500 MHz; ^{13}C 125 MHz). [b] Signals without multiplicity are overlapping ones deduced by HSQC experiments. [c] Data are based on HSQC and HMBC experiments.

cal spin systems for the A (CH_2–CH_2), B (CH–CH_2–CH), and C (CH–CH_2–CH_2) rings of a triterpene scaffold. The other observed spin system from H-15 to CH_3-28 (CH_2–CH_2–CH–CH–CH_3) and CH-21 (CH_2–CH_2–CH–CH_2–CH_2) characterizes the partial structure of ring D with an unusual substituent rearrangement[3] and an olefinic side chain. The HMBC spectrum provides correlations that support substructures A–D and gives information about the regiochemistry of compound **1** (see Figure, Section A3 in the Supporting Information). Thus, $^3J_{H,C}$ correlations of *gem*-dimethyl groups at $\delta_H = 1.07$ and 1.14 ppm with quaternary carbon atoms at $\delta_C = 52.3$ (C5) and 216.7 ppm indicate that the carbonyl group is at C3. The secondary alcohol is sited at C15, as observed by $^{2,3}J_{H,C}$ correlations from the signal at $\delta_H = 4.20$ ppm with carbon atoms C14, C8, C17, and C26. In addition, $^{2,3}J_{H,C}$ correlations from H7 ($\delta_H = 5.83$ ppm) to 6-CH_2, 9-CH, and 5-CH, and those from H21 ($\delta_H = 5.11$ ppm) to 29-CH_3, 30-CH_3, 20-CH_2, 19-CH_2, and C22 define the two trisubstituted double bonds at Δ^7 and Δ^{21}.

The relative configuration of **1** was derived from a combined analysis of $^3J_{H,H}$ coupling constants and NOE correlations (Figure 2 and Table A4 in the Supporting Information). The large 1,2-*trans*-diaxial $J_{15ax,16ax} = 9.2$ Hz coupling along with a correlation from H15 to 27-CH_3 further support the relative orientation of the oxymethine proton at C15 as α, which indicates a β-equatorial disposition for the hydroxy group. Similarly, the orientation of 18-CH_3 and the side chain at C17 were assigned as α and β, respectively, based on correlations of H18/26-CH_3 and H17/27-CH_3. The established structure for compound **1** consists of a carbon skeleton that belongs to a new class of 6/6/6/6 tetracylic triterpenoid: the montecrinane skeleton.[40] Thus, montecrinane A (**1**) is the first example of a

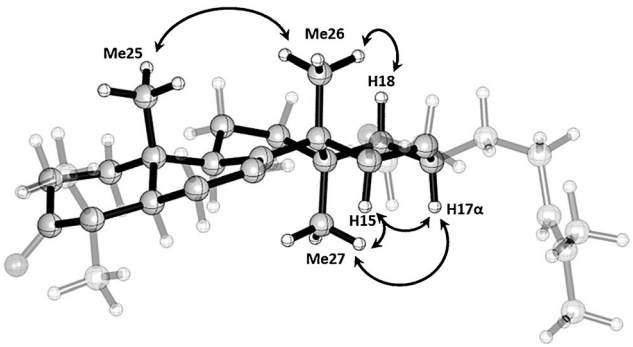

Figure 2. Selected spatial correlations observed in a ROESY experiment ($CDCl_3$, 500 MHz) of compound **1**.

metabolite with this unusual backbone, and its structure was assigned as 15β-hydroxy-3-oxo-montecrinan-7,21-diene (Figure 1).

Montecrinane B (**2**) was isolated as a colorless amorphous solid. It had a specific rotation of −53.1 (*c* 0.22, $CHCl_3$) and the molecular formula was determined as $C_{30}H_{50}O_2$ by HR-ESIMS (calcd: *m/z* 442. 3811; found: *m/z* 442.3799). The IR spectrum shows an absorption band at $\tilde{\nu}=3401\ cm^{-1}$ that is characteristic of hydroxy groups. Based on the ^1H and ^{13}C NMR spectroscopy data (Table 1 and Table A5 in the Supporting Information), compound **2** is a tetracylic-type triterpenoid related to **1**. The main difference is that the resonance of the carbonyl group at C3 in **1** ($\delta_C=216.7$ ppm (s)) is replaced by those of an oxymethine in **2** ($\delta_C=79.2$ ppm (d); $\delta_H=3.27$ ppm (1H, dd, $J_{3\alpha,2\alpha}=3.9$ Hz, $J_{3\alpha,2\beta}=11.3$ Hz)). This suggests that compound **2** is the reduced derivative of **1**, as verified by 2D NMR spectroscopy data (Figure A6 in the Supporting Information). In particular, long-range $^3J_{C,H}$ correlations between the oxymethine carbon signal at $\delta_C=79.2$ ppm and those of 23-CH_3 ($\delta_H=$ 1.00 ppm), 24-CH_3 ($\delta_H=0.89$ ppm), H5 ($\delta_H=1.56$ ppm), and H1 ($\delta_H=1.15$ and 1.69 ppm) were observed in the HMBC experiment. The relative configuration of the oxymethine proton was established on the basis of the coupling constants. Moreover, it was also supported by a ROESY experiment, which showed an NOE with 23-CH_3 and H5; this indicated an axial position for H3 on the α face and an equatorial orientation for the hydroxy group on the β face. These data support the structure of compound **2** as 3β,15β-dihydroxy-montecrinan-7,21-diene.

The molecular formula of montecrinane C (**3**) was deduced as $C_{30}H_{50}O_3$ by HR-ESIMS and ^{13}C NMR spectroscopy data, which indicated the presence of two fewer hydrogen atoms and one more oxygen atom than those in **2**. The ^{13}C NMR spectroscopy data of **3** show two oxygenated carbon atoms at $\delta_C=214.8$ and 76.2 ppm, which exhibit long-range $^{2,3}J_{C,H}$ correlations with H20 ($\delta_H=2.51$ and 2.60 ppm), 29-CH_3 ($\delta_H=$ 1.41 ppm), and 30-CH_3 ($\delta=1.41$ ppm). This pattern of signals is in agreement with the presence of a ketone and a tertiary alcohol group at C21 and C22, respectively. A complete set of 2D NMR spectra (COSY, ROESY, HSQC, and HMBC) was acquired (see Figures A8–A10 in the Supporting Information) to gain the complete and unambiguous assignment of the ^1H and ^{13}C NMR resonances listed in Table 1. These data allowed us to establish the structure of compound **3** as 3β,22-dihydroxy-21-oxo-montecrinan-7-ene.

The absolute configuration of stereocenter C3 of montecrinane C (**3**) was determined by NMR spectroscopy with (*R*)-(−)-α-methoxyphenylacetic acid (MPA) as a chiral derivatizing agent. The MPA ester **3a** was prepared by following Riguera's method.[41] The assignment of the *R*/*S* configuration was based on the space-oriented anisotropic effect produced by the aromatic group that selectively affected substituents of the secondary chiral alcohol (Figure 3 and Tables A11–A14 in the Supporting Information). The ^1H NMR chemical shifts of ester **3a** were assigned based on 2D NMR spectra (COSY and HMBC). A comparative analysis of the ^1H NMR spectroscopy data before and after saturation of the sample with $Ba(ClO_4)_2$ indicated a positive $\Delta\delta$ value for H2 and a negative one for 24-CH_3; this proved the *S* configuration for chiral center C3. Configuration of the remaining stereocenters C5, C9, C10, C13, C14, C17, and C18 were further assigned as *S*, *R*, *S*, *S*, *S*, *R*, *S*, and *R*, respectively, from the aforementioned spectroscopic data of **3**. Attempts to determine the absolute configuration of montecrinanes A (**1**) and B (**2**) by the above methodology was unsuccessful; thus, they were assumed based on biosynthetic considerations, since they contained the same triterpenoid core and specific rotation sign as montecrinane C (**3**).

Biosynthetic proposal for montecrinanes

Plant triterpenoids biogenetically originate from 2,3*S*-oxidosqualene through cation–olefin cyclization, which is the first diversifying step in triterpenoid biosynthesis.[1,24] Stable secondary metabolites are released in the final reaction step by deprotonation, water addition, or oxidation, leading to a wide array of different scaffolds. A key intermediate in the biosynthesis of triterpenoids is the dammarenyl cation (**13**),[42] which is formed by cyclization of 2,3*S*-oxidosqualene with a specific chair–chair–chair–boat conformation (Scheme 1). The D-ring expansion of cation **13** through C16 migration led to a tetracyclic secondary cation: the baccharenyl cation (**14**). Thus, secondary cation **14** is responsible for the formation of tetra- and pentacyclic scaffolds,[5,24,43–45] and this seems to be exceptional when compared with the large number of terpenes obtained via tertiary carbocations.[46]

Intramolecular cyclization of **14** through E-ring closure to the β-face of C18 by the olefinic bond generates the lupenyl cation (**15**). This cation is the key intermediate for the formation of pentacyclic triterpenes (Scheme 2, pathway I). However, the biogenesis of 6/6/6/6 tetracyclic triterpenes occurs from **14** through friedo rearrangement by alternative pathways through 1,2-hydride and methyl shifts.[1,20] For instance, the 1,2-hydride shift from C13 to C18 in carbocation **14**, and successive rearrangements, lead to the *D*:*B*-friedobaccharenyl cation (**21**; Scheme 2, pathway II). The subsequent deprotonation of **21**

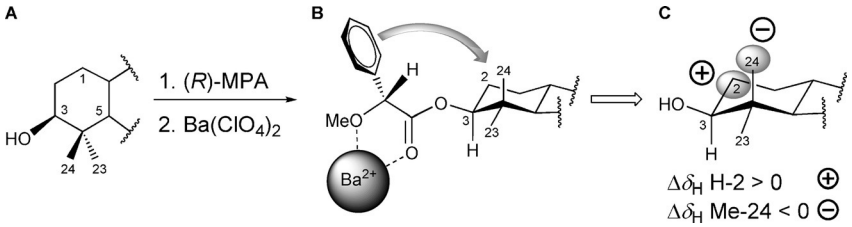

Figure 3. Determination of the absolute configuration of the chiral center C3 in compound **3** from the $\Delta\delta_H^{Ba}$ experimental values of the (*R*)-MPA derivative.

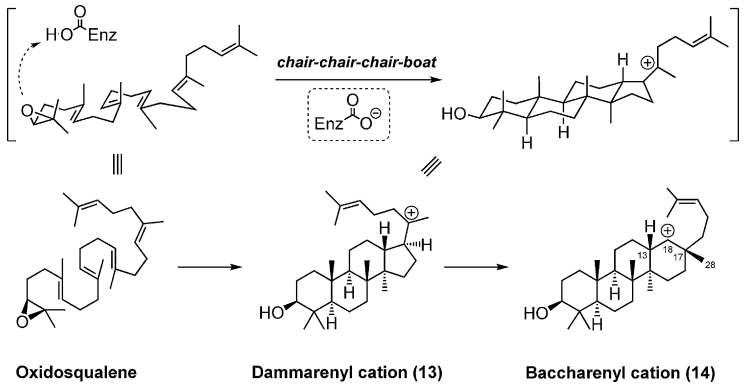

Scheme 1. Cyclization and rearrangement of oxidosqualene to form the dammarenyl cation (**13**); a key intermediate in the biosynthesis of tetra- and pentacyclic triterpenes. Enz = enzyme.

from C6 gives *D*:*B*-friedobaccharan-5,21-diene triterpenes, such as leonal and **4**.[13] On the other hand, the formation of the unprecedented tetracyclic montecrinane skeleton can also be rationalized from intermediate **14**. The novel reaction step in the biosynthesis of the montecrinane framework (**28**) is the 1,2-methyl (28-CH_3) shift from C17β to C18, which generates a more stable tertiary carbocation at C17 (intermediate **23**; Scheme 2, pathway III).

A further 1,2-hydride shift (H18α to C17) leads to intermediate **24**, in which a new stereocenter at C17 is generated.[42] The stereochemistry of the new chiral center locates the side chain in the β position, which is in agreement with experimental observations. As a result, cation **24** is an epimeric intermediate compared with **14** and *D*:*B*-friedobaccharane derivatives. In the next reaction steps, 1,2-hydride shift (H13 to C18) and further methyl shifts (27-CH_3 to C13 and 26-CH_3 to C14) lead to the montecrinanyl cation (**27**), with a positive charge at C8. Subsequent deprotonation at C7 generates a new 6/6/6/6 tetracyclic triterpenene skeleton: montecrinane **28**. Selective oxidation at C3 and hydroxylation at C15 lead to montecrinanes A (**1**) and B (**2**). Moreover, epoxidation of the Δ^{21}-double bond followed by epoxide ring opening and water addition gave rise to montecrinane C (**3**).

Theoretical studies on 6/6/6/6-tetracyclic triterpene biosynthesis

Quantum chemical calculations have been used to describe terpene-forming carbocation rearrangements, to predict geometric structures and relative energies of intermediates and transition-state structures, as well as to support new biosynthetic pathways. Among DFT methods, the B3LYP functional has become the most common method employed to calculate the geometries of carbocation precursors of terpenes. Particularly, B3LYP geometries and mPW1PW91 single-point energies (mPW1PW91/6-31 + G(d,p)//B3LYP/6-31 + G(d,p) methods) have been successfully used by Matsuda et al.[43] and Tantillo[25] to compute carbocation reactions in the biosynthesis of natural products.[26,47–49]

To obtain mechanistic insights into the 6/6/6/6 tetracyclic triterpene biosynthesis, theoretical studies were carried out to compare the energetic profile of the possible pathways that led to these triterpenes, starting from **14** (Scheme 2). Therefore, this study focuses on the feasibility of the formation of cations **21** and **27** to understand energetic factors involved in the mechanisms of tetracyclic triterpene skeleton formation. Additionally, the formation of **15** from carbocation **14** was studied because lupane-type triterpenes (compounds **7**–**12**) were also isolated from *C. vulcanicola*.

First, a conformational study of **14** was carried out by using PcModel 9.2.[50] Then, the minimized structures were optimized at the B3LYP/6-31 + G(d,p) level of theory in the gas phase by using Gaussian 09.[51] The B3LYP functional tends to underestimate the relative stability of cyclic structures. Therefore, single-point energy calculations were performed at the mPW1PW91/6-31 + G(d,p) level of theory by using the B3LYP geometries, and the results were compared with those obtained by using the M06-2X/6-311 + G(d,p)//B3LYP/6-31 + G(d,p) method.[52,53]

Conformational analysis shows that secondary carbocation **14** might exist as a true minimum in the potential energy surface. From this structure, a sequence of rearrangements (1,2-hydride or -methyl shifts) were studied to compare the energetic changes of the proposed biosynthetic pathways. The results of these calculations are summarized in the energy diagrams shown in Figure 4. The gas-phase model for the montecrinane framework formation is presented in Figure 4A. The Gibbs free energy profile shows that the 1,2-methyl shift from **14** to tertiary carbocation **23** is the rate-determining step of the process. The activation energy of this step (**TS-1**) is $\Delta G^{\ddagger}_{298} = 10.2$ kcal mol^{-1}. Subsequent rearrangements from intermediate **23** lead to the formation of **27**, which takes place due to the high stability of the tertiary carbocations involved in the rearrangements (intermediates **23**–**27**) and the small activation barriers for their formation (**TS-2**, **TS-3**, **TS-4**, and **TS-5**). The 1,2-hydride shift from carbocation **14** to tertiary carbocation **16**, and subsequent rearrangements, generate the *D*:*B*-friedobaccharane skeleton (Figure 4B). The activation energy of the 1,2-hidryde shift (**TS-6**) is $\Delta G^{\ddagger}_{298} = 6.3$ kcal mol^{-1}, which is 3.9 kcal mol^{-1} lower than that of **TS-1**. This energetic difference could be due to the nature of the migration of the species (hydride or methyl group) involved in the rearrangement reaction. For hydride migration, there are interactions with the s orbital of the hydride, whereas in the case of methyl migration sp^3 orbitals are involved. The rate-determining step of the whole process of going from **14** to **21** has an energetic barrier of $\Delta G^{\ddagger}_{298} = 8.5$ kcal mol^{-1} (**TS-10**), which is similar to that of **TS-1** ($\Delta G^{\ddagger}_{298} = 10.2$ kcal mol^{-1}). Based on the similar energetic profiles predicted by theoretical calculations, the two triterpene frameworks could occur in nature.

Finally, the reaction path connecting **14** and **15** was studied and compared with previous mechanisms (Scheme 3). In secondary carbocation **14**, the double bond of the side chain is located in the proximity of the carbon with electron deficiency

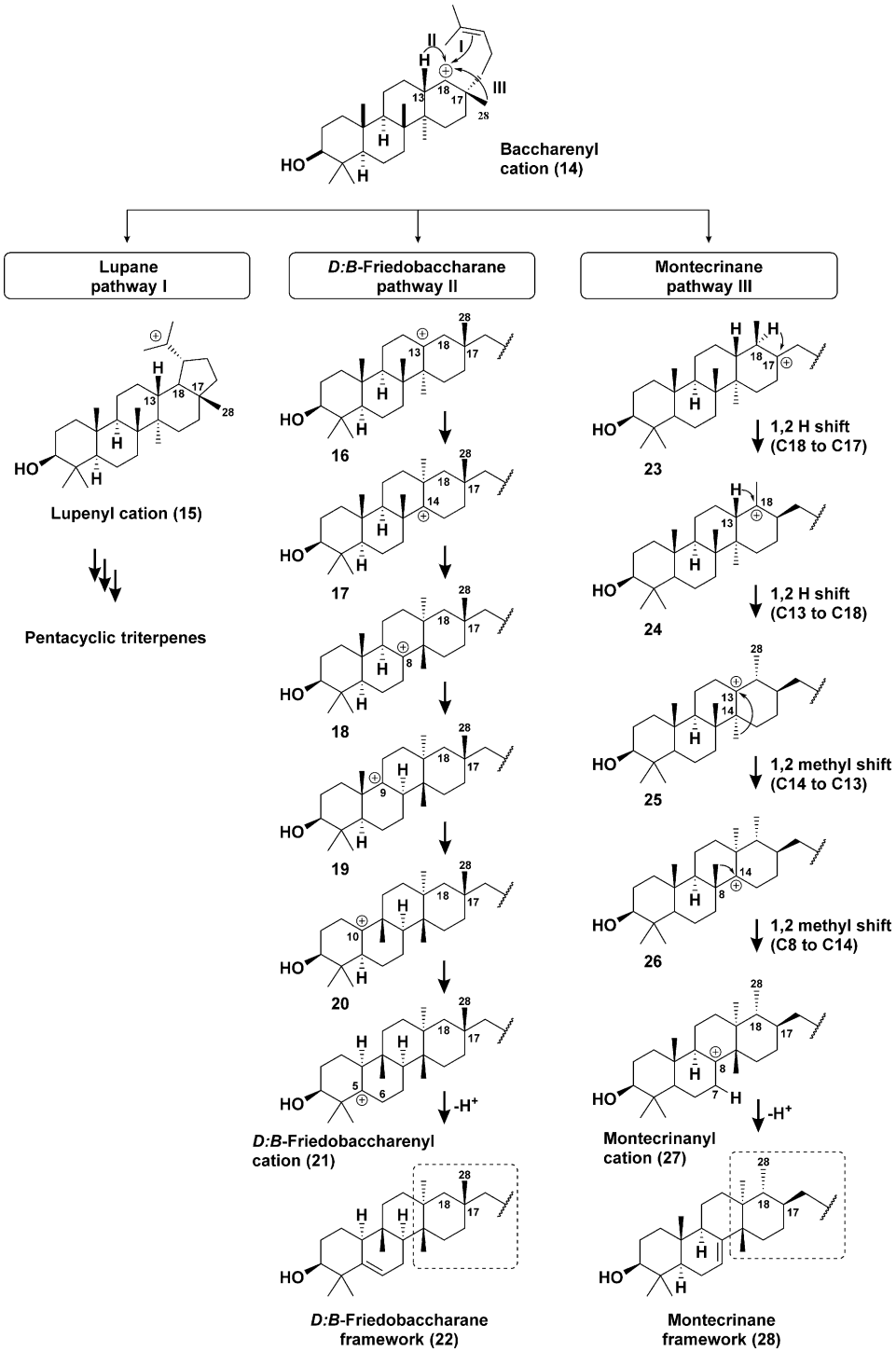

Scheme 2. Proposed reaction mechanism to form the montecrinane framework as an alternative pathway to the biosynthesis of lupane and *D:B*-friedobaccharene skeletons.

(C18). The intramolecular cation–π interaction[54,55] between the secondary cation substructure (C18) and the C21=C22 π bond preorganize **14** for the cyclization reaction, which takes place with a low activation barrier ($\Delta G^{\ddagger}_{298} = 0.9$ kcal mol^{-1}). Due to structural similarity between carbocation **14** and the transition state (**TS-12**) of pathway I, no energetic barrier should be expected for this process; this indicates that **14** is a metastable carbocation, which is typical of secondary carbocations.[43]

The competitive mechanisms presented in Scheme 3 indicate that **14** can be transformed into **15**, which is obtained through the most favorable process (kinetically and thermodynamically). Thus, the formation of carbocation **14** and the rearrangements involved in the biosynthesis of baccharane-derived

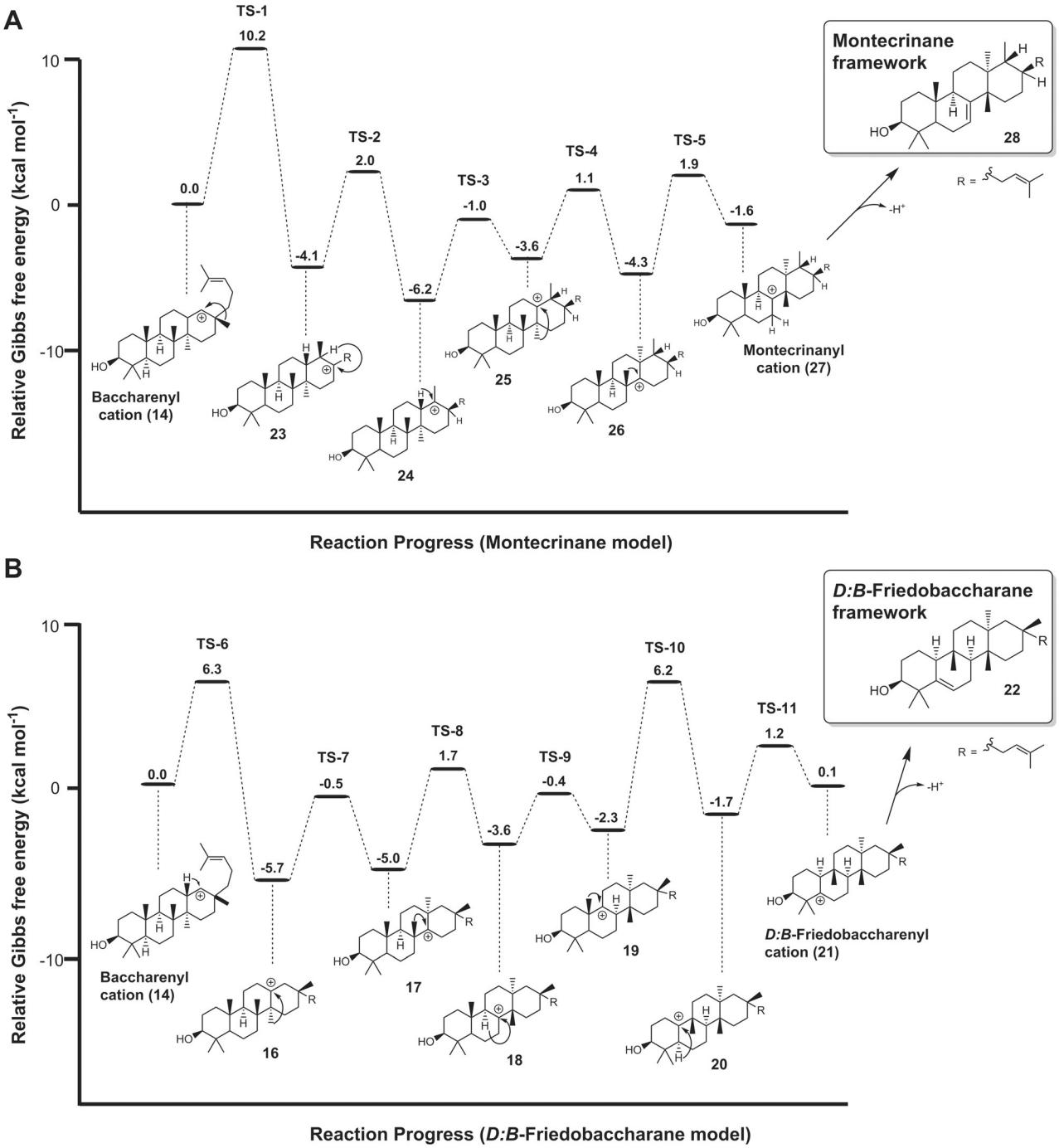

Figure 4. Relative Gibbs free energy ($\Delta G^{\ddagger}_{298}$ in kcal mol^{-1}) profile predicted at the mPW1PW91/6-31 + G(d,p)//B3LYP/6-31 + G(d,p) level of theory for montecrinane (A) and *D*:*B*-friedobaccharane (B) framework formation. Geometries, energies, and a comparison of mPW1PW91 and M06-2X functionals are given in the Supporting Information.

terpenoids will depend on the enzymes present in the reaction media.[56,57] For instance, a specific OSC, such as synthases reported for related metabolites,[58,59] could be responsible for the formation of an unprecedented backbone in one sequence of catalytic steps. Overall, the activation energies of the rate-determining steps connecting **14** with cations **15** (0.9 kcal mol^{-1}), **21** (8.5 kcal mol^{-1}), and **27** (10.2 kcal mol^{-1}) are consistent with the relative abundance of the lupane (**7**–**12**), *D*:*B*-friedobachharane (**4**–**6**), and montecrinane (**1**–**3**) triterpenes described herein (see Table A15 in the Supporting Information).

Conclusion

Complete carbocation cyclization/rearrangement pathways from **14** to montecrinane and *D*:*B*-friedobaccharane frameworks were developed on the basis of the results of DFT calculations. In the proposed mechanism towards montecrinanes,

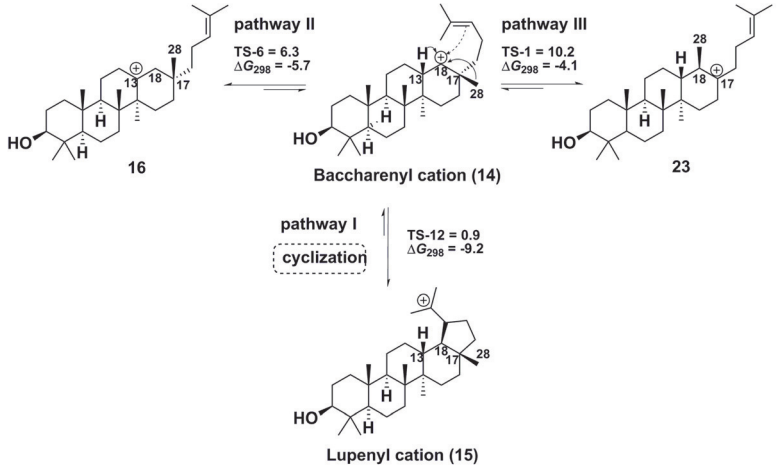

Scheme 3. Competitive reaction pathways from the baccharenyl cation (**14**) to tetra-/pentacyclic skeletons. Energies [kcal mol^{-1}] are given at the mPW1PW91/6-31 + G(d,p)//B3LYP/6-31 + G(d,p) level of theory.

the first reaction step is a novel methyl shift from C17 to C18, which generates a tertiary carbocation at C17. Afterward, 1,2-hydride shift from C18 to C17 changes the configuration of the side chain at C17. Subsequent rearrangements generate the montecrinanyl cation, and the final step of the process is the elimination of a proton from C7. The montecrinane skeleton might be indicative of a divergent pathway for tetracyclic triterpene biosynthesis from **14**. The proposed biosynthetic pathway is energetically feasible; therefore, more secondary metabolites containing this skeleton are expected to be isolated from Celastraceae species. The co-occurrence of *D*:*B*-friedobaccharanes supports the hypothesis that Celastraceae species and, in particular, *C. vulcanicola*, possess specific OSCs that lead to the biosynthesis of uncommon 6/6/6/6 tetracyclic triterpenoids. Hence, 1,2-methyl and -hydride shifts proposed for the biosynthesis of montecrinanes might require a specific OCS capable of stabilizing carbocation intermediates.

Experimental Section

General

Optical rotations were measured on a PerkinElmer 241 automatic polarimeter in $CHCl_3$ at 20 °C. UV spectra were obtained on a JASCO V-560 spectrophotometer in absolute EtOH. IR (film) spectra were measured on a Bruker IFS 55 spectrophotometer. ^{1}H (500 MHz) and ^{13}C NMR (125 MHz) spectra were recorded on a Bruker Avance 500 spectrometer at 25 °C; chemical shifts were referenced to the residual solvent signal ($CDCl_3$: $\delta_H = 7.26$ ppm, $\delta_C = 77.0$ ppm); DEPT, TOCSY, COSY, ROESY (spin lock field 2500 Hz), HSQC, and HMBC (optimized for $J = 7.7$ Hz) experiments were carried out with the pulse sequences given by Bruker. EIMS and HR-EIMS were obtained on a Micromass Autospec spectrometer, and HR-ESIMS spectra (positive mode) were performed on LCT Premier XE Micromass electrospray spectrometer. Silica gel 60 (particle size 15–40 and 63–200 μm, Machery-Nagel) and Sephadex LH-20 (Pharmacia Biotech) were used for column chromatography, whereas silica gel 60 F_{254} (Machery-Nagel) was used for analytical and preparative TLC. Centrifugal planar chromatography was performed by means of a Chromatotron instrument (model 7924T, Harrison Research Inc., Palo Alto, CA, USA) on manually coated silica gel 60 GF254 (Merck) by using a 1, 2, or 4 mm plates. The spots were visualized by UV light and heating silica gel plates sprayed with H_2O/H_2SO_4/AcH (1:4:20). All solvents used were of analytical grade (Panreac). Optically pure MPA was purchased from Sigma, whereas the other reagents were purchased from Aldrich and used without further purification.

Plant material

C. vulcanicola J. (Donnell Smith; Celastraceae) was collected in November 2009 at Montecristo National Park (2051 m above sea level), in the municipality of Metapán, Province of Santa Ana, El Salvador. The plant was identified by Jorge Alberto Monterrosa Salomón, Curator of the Herbarium at the Jardín Botánico, La Laguna, El Salvador, and a voucher specimen (J. Monterrosa & R. Carballo 412) was deposited in the Herbarium of Missouri Botanical Garden, St. Louis, MO, USA.

Extraction and isolation

The air-dried and powdered root bark of *C. vulcanicola* (0.8 kg) was extracted with *n*-hexane/Et_2O (1:1, 4.0 L, 48 h) in a Soxhlet apparatus. Evaporation of the solvent under reduced pressure provided the crude extract (24.0 g), which was subjected to column chromatography over silica gel (1.0 kg, 70–230 mesh) by using increasing polarity mixtures of hexanes/EtOAc (0–100%, 34.0 L) as the eluent to afford nine fractions (1–9). Fraction 2 (2.3 g; hexanes/EtOAc, 8:2) was separated by chromatography on Sephadex LH-20 (hexanes/$CHCl_3$/MeOH, 2:1:1, 2.5 L) to afford 26 fractions, which were combined into six fractions (2a–f) on the basis of their TLC profiles. Fractions 2b (480.0 mg), 2c (608.0 mg), and 2f (127.0 mg) were further subjected to centrifugal planar chromatography on silica gel by using mixtures of CH_2Cl_2/Me_2CO of increasing polarity (10.0 to 8:2) to afford five (2b1–5), eight (2c1–8) and four (2f1–4) subfractions, respectively. Subfractions 2b2, 2c7, and 2f3 were further purified by preparative TLC by using mixtures of hexanes/EtO_2 (8:2), CH_2Cl_2/Me_2CO (9:1), and toluene/EtOAc (7:3), respectively, to yield compounds **1** (3.8 mg), **2** (2.2 mg), and **3** (9.7 mg), in addition to the known compounds, **4** (8.5 mg), **5** (5.0 mg), and **6** (3.9 mg). Fraction 5 (1.6 g; hexanes/EtOAc, 7:3) was separated by chromatography on Sephadex LH-20 (hexanes/$CHCl_3$/MeOH, 2:1:1), on silica gel (hexanes/EtOAc of increasing polarity, 8:2 to 3:7), by centrifugal

planar chromatography (CH_2Cl_2/Me_2CO of increasing polarity, 9:1 to 7:3) and by preparative HPTLC (hexanes/Et_2O, 3:7) to give the known lupane triterpenes **7**[36] (6.2 mg), **8**[36] (4.8 mg), **9**[37] (7.2 mg), **10**[36] (12.6 mg), **11**[36] (7.8 mg), and **12**[38] (4.1 mg).

Montecrinane A (1)

Colorless amorphous solid; $[\alpha]_D^{20>} = -58.6^\circ$ ($c = 0.38$ in $CHCl_3$); for ^1H and ^{13}C NMR data, see Table 1; for 2D spectra, see Figures A2–A4 in the Supporting Information; IR (film) $\nu = 3455$, 2924, 2855, 1708, 1459, 1381, 1267, 1046, 971, 755, 573 cm^{-1}; EIMS: *m/z* (%): 440 (18) [M^+], 422 (4) [$M^+ - 18(H_2O)$], 407 (19), 353 (6), 323 (9), 287 (22), 273 (20), 257 (17), 245 (18), 231 (45), 203 (11), 185 (13), 159 (27), 149 (26), 133 (38), 119 (48), 109 (78), 105 (44), 95 (68), 69 (100), 55 (95); HR-EIMS: *m/z* calcd for $C_{30}H_{48}O_2$ [M^+]: 440.3654; found: 440.3654.

Montecrinane B (2)

Colorless amorphous solid; $[\alpha]_D^{20>} = -53.1^\circ$ ($c = 0.22$ in $CHCl_3$); for ^1H and ^{13}C NMR data, see Table 1; for 2D spectra, see Figure A6 in the Supporting Information; IR (film) $\nu = 3401$, 2923, 2853, 1460, 1378, 1270, 1027, 974, 755, 501 cm^{-1}; EIMS: *m/z* (%): 442 (4), 424 (7) [$M^+ - 18(H_2O)$], 407 (8), 289 (9), 215 (20), 187 (32), 173 (30), 161 (24), 145 (31), 121 (59), 109 (86), 107 (64), 105 (44), 95 (81), 69 (99), 55 (100); HR-EIMS: *m/z* calcd for $C_{30}H_{50}O_2$ [M^+]: 442.3811; found: 442.3799.

Montecrinane C (3)

Colorless amorphous solid; $[\alpha]_D^{20>} = -12.5^\circ$ ($c = 0.97$ in $CHCl_3$); for ^1H and ^{13}C NMR data, see Table 1; for 2D spectra, see Figures A8–10 in the Supporting Information; IR (film) $\nu = 3436$, 2927, 2872, 1709, 1462, 1377, 1279, 1166, 1067, 1033, 756 cm^{-1}; HR-ESIMS: *m/z* calcd for $C_{30}H_{49}O_3$ [$M^+ - Na - H$]: 472.3682; found: 472.3682.

Preparation of (*R*)-(−)-α-methoxyphenylacetic ester (3 a)

A solution of (*R*)-MPA (5.0 mg), **3** (3.8 mg), dicyclohexylcarbodiimide (DCC; 6.0 mg), and 4-dimethylaminopyridine (DMAP; 5.3 mg) in dry dichloromethane (1 mL) was stirred at room temperature and under a nitrogen atmosphere for 24 h. The reaction mixture was filtered through a short cotton-wool filter and the solvent was removed under reduced pressure to give a thick oil, which was purified by preparative TLC on silica gel (*n*-hexane/EtOAc, 8:2) to give the analytically pure ester **3 a** (2.4 mg) as an amorphous solid. ^1H NMR (CD_3CN, 500 MHz): $\delta = 0.63$ (d, $J = 6.5$ Hz, 3H; 28-CH_3), 0.73 (s, 3H; 25-CH_3), 0.77 (s, 3H; 27-CH_3), 0.78 (s, 3H; 24-CH_3), 0.90 (s, 3H; 23-CH_3), 0.95 (s, 3H; 26-CH_3), 1.33 (s, 3H; 29-CH_3), 1.42 (s, 3H; 30-CH_3), 1.42 (m, 1H; H2β), 1.48 (m, 1H; H2α), 3.37 (s, 3H; OMe-MPA), 4.52 (dd, $J = 4.4$, 11.7 Hz, 1H; H3), 4.83 (s, 1H; H2′-MPA), 5.24 (dd, $J = 3.2$, 6.3 Hz, 1H; H7), 7.21–7.48 ppm (m, 5H; MPA); ^{13}C NMR (CD_3CN, 500 MHz): $\delta = 12.1$ (q, C25), 14.8 (q, C24), 17.4 (q, C28), 18.1 (t, C11), 21.3 (q, C26), 22.3 (q, C29), 22.4 (q, C30), 23.3 (t, C6), 24.4 (t, C2), 26.3 (q, C23), 26.4 (q, C26), 27.1 (t, C16), 28.9 (t, C19), 31.6 (t, C20), 33.2 (t, C12), 33.3 (t, C15), 34.3 (s, C10), 35.0 (d, C17), 35.8 (t, C1), 37.4 (s, C4), 43.6 (s, C13), 48.1 (d, C9), 49.9 (d, C5), 50.6 (s, C14), 52.4 (d, C18), 81.2 (d, C3), 84.4 (s, C22), 115.8 (d, C7), 145.6 (s, C8), 208.3 ppm (s, C21); MPA [56.4 (q), 82.2 (d), 126.6 (d), 128.0 (2×d), 128.7 (2×d), 134.9 (s), 171.2 ppm (s)]; ^1H NMR (CD_3CN, 500 MHz, saturated with $Ba(ClO_4)_2$): $\delta = 0.63$ (s, 3H; 28-CH_3), 0.64 (s, 3H; 25-CH_3), 0.74 (s, 3H; 27-CH_3), 0.82 (s, 3H; 24-CH_3), 0.86 (s, 3H; 23-CH_3), 0.91 (s, 3H; 26-CH_3), 1.15 (m, 1H; H2β), 1.24 (m, 1H; H2α), 1.30 (s, 3H; 29-CH_3), 1.48 (s, 3H; 30-CH_3), 3.32 (s, 3H; OMe-MPA), 4.54 (dd, $J = 3.9$, 11.5 Hz, 1H; H3), 5.08 (s, 1H; H2′-MPA), 5.21 (dd, $J = 3.6$, 6.0 Hz, 1H; H7), 7.39–7.51 ppm (m, 5H; MPA); ^{13}C NMR (CD_3CN, 500 MHz, saturated with $Ba(ClO_4)_2$): $\delta = 13.5$ (q, C25), 14.9 (q, C24), 18.1 (t, C11), 18.5 (q, C28), 21.8 (q, C27), 21.9 (q, C30), 23.1 (q, C29), 23.5 (t, C6), 24.3 (t, C2), 26.7 (q, C23), 26.9 (q, C26), 27.1 (t, C16), 28.8 (t, C19), 31.7 (t, C20), 33.1 (t, C12), 33.6 (t, C15), 34.4 (s, C10), 34.4 (d, C17), 35.4 (t, C1), 37.4 (s, C4), 43.1 (s, C13), 49.2 (d, C9), 50.1 (d, C5), 50.9 (s, C14), 52.2 (d, C18), 84.1 (d, C3), 86.9 (s, C22), 118.3 (d, C7), 145.7 (s, C8), 209.7 ppm (s, C21); MPA (56.0 (q), 82.4 (d), 126.6 (d), 128.0 (2×d), 128.6 (2×d), 135.0 (s), 171.1 ppm (s)); for ^1H, ^{13}C NMR, and 2D NMR spectra, see Figures A11, A12, and A14, respectively, in the Supporting Information,.

Computational details

The conformational space was searched by GMMX (included in PcModel 9.2[50]) by using a mixed method, which allowed the program to 1) randomly select a subset of all bonds for rotation; and 2) randomly move a subset of all heavy and non-volatile atoms in 3D space, which caused small changes in the shape of the molecule. The minimized structures obtained with PcModel 9.2[50] were reoptimized at the B3LYP/6–31+G(d,p) level of theory by using Gaussian 09.[51] The geometric optimizations of ground and transition states (as a first-order saddle point) and reaction profiles were performed without any symmetry restrictions. Harmonic vibrational frequency calculations were performed analytically to verify the character of the stationary point obtained and to correct energies for the zero-point vibrations. Transition states were fully optimized and characterized by the presence of only one imaginary frequency. Notably, no basis set superposition error (BSSE) correction was carried out during reaction profiles because hydride (or methyl group) transfer occurred in the same molecule. Optimized coordinates and energies of all structures are included in the Supporting Information. Images were produced by using the CYL view program.[60]

Acknowledgements

This work was supported by the FP7-REGPOT-2012-CT2012-316137-IMBRAIN and CTQ2011-28417-C02-01 (MINECO) projects. We thank Jorge A. Monterrosa for collecting and identifying the plant material, and the Servicio de Parques Nacionales y Vida Silvestre, Dirección de Recursos Renovables del Ministerio de Agricultura y Ganadería (MAG), and Fundación Ecológica de El Salvador (SALVANATURA) for supplying the plant material. A.E.A. thanks CONICYT and FONDECYT 3160414 of Chile for a fellowship.

Keywords: biosynthesis · density functional calculations · natural products · structure elucidation · terpenoids

[1] R. Xu, G. C. Fazio, S. P. T. Matsuda, *Phytochemistry* **2004**, *65*, 261–291.
[2] R. A. Hill, J. D. Connolly, *Nat. Prod. Rep.* **2015**, *32*, 273–327.
[3] H. Sheng, H. Sun, *Nat. Prod. Rep.* **2011**, *28*, 543–593.
[4] F. Mo, T. Anthonsen, T. Brunn, *Acta Chem. Scand.* **1972**, *26*, 1287–1288.
[5] M. Shibuya, A. Sagara, A. Saitoh, T. Kushiro, Y. Ebizuka, *Org. Lett.* **2008**, *10*, 5071–5074.
[6] N. Shoji, A. Umeyama, Z. Taira, T. Takemoto, K. Nomoto, K. Mizukawa, Y. Ohizumi, *J. Chem. Soc. Chem. Commun.* **1983**, *16*, 871–873.
[7] L. Pan, L. B. S. Kardono, S. Riswan, D. J. Newman, D. Kinghorn, *J. Nat. Prod.* **2010**, *73*, 1873–1878.

[8] B. Y. Hwang, B. N. Su, H. Chai, Q. Mi, L. B. S. Kardono, D. Kinghorn, *J. Org. Chem.* **2004**, *69*, 3350 – 3358.
[9] N. Stiti, S. Triki, M-A. Hartmann in *Olives and Olive Oil in Heat and Disease Prevention* (Eds: V. R. Preedy, R. R. Watson), Elsevier, London, **2010**, pp. 211 – 218.
[10] T. Fujioka, Y. Kashiwada, H. Okabe, K. Mihashi, K.-H. Lee, *Bioorg. Med. Chem. Lett.* **1996**, *6*, 2807 – 2810.
[11] K. Masuda, K. Shiojima, H. Ageta, *Chem. Pharm. Bull.* **1983**, *31*, 2530 – 2533.
[12] S. Öksüz, S. Serin, *Phytochemistry* **1997**, *46*, 545 – 548.
[13] M. J. Núñez, M. R. López, I. A. Jiménez, L. M. Moujir, A. G. Ravelo, I. L. Bazzocchi, *Tetrahedron Lett.* **2004**, *45*, 7367 – 7370.
[14] Y. Zhang, S. Nakamura, T. Wang, H. Matsuda, M. Yoshikawa, *Tetrahedron* **2008**, *64*, 7347 – 7352.
[15] T. Akihisa, K. Yasukawa, Y. Kimura, S. Takase, S. Yamanouchi, T. Tamura, *Chem. Pharm. Bull.* **1997**, *45*, 2016 – 2023.
[16] T. Akihisa, E. M. K. Wijeratne, H. Tokuda, F. Enjo, M. Toriumi, Y. Kimura, K. Koike, T. Nikaido, Y. Tezuka, H. Nishino, *J. Nat. Prod.* **2002**, *65*, 158 – 162.
[17] R. Fröde, M. Bröckelmann, B. Steffan, W. Steglich, R. Marumoto, *Tetrahedron* **1995**, *51*, 2553 – 2560.
[18] W. B. Zhou, J. Y. Tao, H. M. Xu, K. Li Chen, G. Z. Zeng, C. J. Ji, Y. M. Zhang, N. H. Tan, *Z. Naturforsch. Sect. B* **2010**, *65*, 1393 – 1396.
[19] M. Shibuya, T. Xiang, Y. Katsube, M. Otsuka, H. Zhang, Y. Ebizuka, *J. Am. Chem. Soc.* **2007**, *129*, 1450 – 1455.
[20] S. Lodeiro, Q. Xiong, W. K. Wilson, M. D. Kolesnikova, C. S. Onak, S. P. T. Matsuda, *J. Am. Chem. Soc.* **2007**, *129*, 11213 – 11222.
[21] S. Sawai, H. Uchiyama, S. Mizuno, T. Aoki, T. Akashi, S-i. Ayabe, T. Takahashi, *FEBS Lett.* **2011**, *585*, 1031 – 1036.
[22] S. C. Roberts, *Nat. Chem. Biol.* **2007**, *3*, 387 – 395.
[23] S. T. Mugford, T. Louveau, R. Melton, X. Qi, S. Bakht, L. Hill, T. Tsurushima, S. Honkanen, S. J. Rosser, G. P. Lomonossoff, A. Osbourn, *Plant Cell* **2013**, *25*, 1078 – 1092.
[24] R. Thimmappa, K. Geisler, T. Louveau, P. O'Maille, A. Osbourn, *Annu. Rev. Plant Biol.* **2014**, *65*, 225 – 257.
[25] D. J. Tantillo, *Nat. Prod. Rep.* **2011**, *28*, 1035 – 1053.
[26] D. J. Tantillo, *Nat. Prod. Rep.* **2013**, *30*, 1079.
[27] N. Alvarenga, E. A. Ferro *in Studies in Natural Products Chemistry, Vol. 33* (Ed.: Atta-ur-Rahman), Elsevier, Amsterdam, **2006**, pp. 239 – 307.
[28] A. A. Osorio, A. Muñoz, D. Torres-Romero, L. M. Bedoya, N. R. Perestelo, I. A. Jiménez, J. Alcamí, I. L. Bazzocchi, *Eur. J. Med. Chem.* **2012**, *52*, 295 – 303.
[29] M. J. Núñez, A. E. Ardiles, M. L. Martínez, D. Torres-Romero, I. A. Jiménez, I. L. Bazzocchi, *Phytochem. Lett.* **2012**, *5*, 244 – 248.
[30] D. Torres-Romero, B. King-Diaz, I. A. Jiménez, B. Lotina-Hennsen, I. L. Bazzocchi, *J. Nat. Prod.* **2008**, *71*, 1331 – 1335.
[31] D. Torres-Romero, F. Muñoz-Martínez, I. A. Jiménez, S. Castanys, F. Gamarro, I. L. Bazzocchi, *Org. Biomol. Chem.* **2009**, *7*, 5166 – 5172.
[32] D. Torres-Romero, I. A. Jiménez, R. Rojas, R. H. Gilman, M. López, I. L. Bazzocchi, *Bioorg. Med. Chem.* **2011**, *19*, 2182 – 2189.
[33] O. Callies, M. P. Sánchez-Cañete, F. Gamarro, I. A. Jiménez, S. Castanys, I. L. Bazzocchi, *J. Nat. Prod.* **2015**, *78*, 736 – 745.
[34] D. Torres-Romero, B. King-Diaz, R. J. Strasser, I. A. Jiménez, B. Lotina-Hennsen, I. L. Bazzocchi, *J. Agric. Food Chem.* **2010**, *58*, 10847 – 10854.
[35] A. E. Ardiles, A. González-Rodríguez, M. J. Nuñez, N. R. Perestelo, V. Pardo, I. A. Jiménez, A. M. Valverde, I. L. Bazzocchi, *Phytochemistry* **2012**, *84*, 116 – 124.
[36] M. J. Núñez, A. E. Ardiles, M. L. Martínez, D. Torres-Romero, I. A. Jiménez, I. L. Bazzocchi, *Phytochem. Lett.* **2013**, *6*, 148 – 151.
[37] M. J. Núñez, C. P. Reyes, I. A. Jiménez, L. Moujir, I. L. Bazzocchi, *J. Nat. Prod.* **2005**, *68*, 1018 – 1021.
[38] A. P. Dantanarayana, N. S. Kumar, M. U. S. Sultanbawa, S. J. Balasubramaniam, *J. Chem. Soc. Perkin Trans. 1* **1981**, 2717 – 2723.
[39] M. Kuroyanagi, M. Shiotsu, T. Ebihara, H. Kawai, A. Ueno, S. Fukushima, *Chem. Pharm. Bull.* **1986**, *34*, 4012 – 4017.
[40] The new compounds were named montecrinanes based on the place of collection of the plant (*C. vulcanicola*), which was Montecristo National Park on the north-western tip of El Salvador.
[41] J. M. R. Seco, E. Quiñoa, R. Riguera, *Chem. Rev.* **2004**, *104*, 17 – 117.
[42] Q. Xiong, F. Rocco, W. K. Wilson, R. Xu, M. Ceruti, S. P. T. Matsuda, *J. Org. Chem.* **2005**, *70*, 5362 – 5375.
[43] S. P. T. Matsuda, W. K. Wilson, Q. Xiong, *Org. Biomol. Chem.* **2006**, *4*, 530 – 543.
[44] W. K. Wilson, R. Xu, M. Ceruti, S. P. T. Matsuda, *J. Org. Chem.* **2005**, *70*, 6492.
[45] I. Abe, Y. Sakano, H. Tanaka, W. Lou, H. Noguchi, M. Shibuya, Y. Ebizuka, *J. Am. Chem. Soc.* **2004**, *126*, 3426 – 3427.
[46] D. J. Tantillo, *Chem. Soc. Rev.* **2010**, *39*, 2847 – 2854.
[47] Y. J. Hong, D. J. Tantillo, *Nat. Chem.* **2009**, *1*, 384 – 389.
[48] Y. J. Hong, D. J. Tantillo, *Org. Lett.* **2011**, *13*, 1294 – 1297.
[49] Y. J. Hong, D. J. Tantillo, *Nat. Chem.* **2014**, *6*, 104 – 111.
[50] PCModel, version 9.2; Serena Software, Bloomington, IN.
[51] Gaussian 09, Revision A.02, M. J. Frisch, G. W. Trucks, H. B. Schlegel, G. E. Scuseria, M. A. Robb, J. R. Cheeseman, G. Scalmani, V. Barone, B. Mennucci, G. A. Petersson, H. Nakatsuji, M. Caricato, X. Li, H. P. Hratchian, A. F. Izmaylov, J. Bloino, G. Zheng, J. L. Sonnenberg, M. Hada, M. Ehara, K. Toyota, R. Fukuda, J. Hasegawa, M. Ishida, T. Nakajima, Y. Honda, O. Kitao, H. Nakai, T. Vreven, J. A. Montgomery, Jr., J. E. Peralta, F. Ogliaro, M. Bearpark, J. J. Heyd, E. Brothers, K. N. Kudin, V. N. Staroverov, R. Kobayashi, J. Normand, K. Raghavachari, A. Rendell, J. C. Burant, S. S. Iyengar, J. Tomasi, M. Cossi, N. Rega, J. M. Millam, M. Klene, J. E. Knox, J. B. Cross, V. Bakken, C. Adamo, J. Jaramillo, R. Gomperts, R. E. Stratmann, O. Yazyev, A. J. Austin, R. Cammi, C. Pomelli, J. W. Ochterski, R. L. Martin, K. Morokuma, V. G. Zakrzewski, G. A. Voth, P. Salvador, J. J. Dannenberg, S. Dapprich, A. D. Daniels, O. Farkas, J. B. Foresman, J. V. Ortiz, J. Cioslowski, and D. J. Fox, Gaussian, Inc., Wallingford CT, **2009**.
[52] Y. Zhao, D. G. Truhlar, *Theor. Chem. Acc.* **2008**, *120*, 215 – 241.
[53] Y. Zhao, D. G. Truhlar, *Acc. Chem. Res.* **2008**, *41*, 157 – 167.
[54] Y. J. Hong, D. J. Tantillo, *Chem. Sci.* **2013**, *4*, 2512 – 2518.
[55] Y. J. Hong, D. J. Tantillo, *Org. Lett.* **2015**, *17*, 5388 – 5391.
[56] Y. J. Hong, D. J. Tantillo, *J. Am. Chem. Soc.* **2011**, *133*, 18249 – 18256.
[57] R. P. Pemberton, K. C. Ho, D. J. Tantillo, *Chem. Sci.* **2015**, *6*, 2347 – 2353.
[58] L. Kürti, R.-J. Chein, E. J. Corey, *J. Am. Chem. Soc.* **2008**, *130*, 9031 – 9036.
[59] Z. Wang, T. Yeats, H. Han, R. Jetter, *J. Biol. Chem.* **2010**, *285*, 29703 – 29712.
[60] CYLview, 1.0b; Legault, C. Y., Université de Sherbrooke, **2009** (http://www.cylview.org).

Received: January 21, 2016
Published online on April 23, 2016